

Model of a fluid at small and large length scales and the hydrophobic effect

Pieter Rein ten Wolde, Sean X. Sun, and David Chandler

Department of Chemistry, University of California, Berkeley, California 94720

(Received 26 June 2001; published 5 December 2001)

We present a statistical field theory to describe large length scale effects induced by solutes in a cold and otherwise placid liquid. The theory divides space into a cubic grid of cells. The side length of each cell is of the order of the bulk correlation length of the bulk liquid. Large length scale states of the cells are specified with an Ising variable. Finer length scale effects are described with a Gaussian field, with mean and variance affected by both the large length scale field and by the constraints imposed by solutes. In the absence of solutes and corresponding constraints, integration over the Gaussian field yields an effective lattice-gas Hamiltonian for the large length scale field. In the presence of solutes, the integration adds additional terms to this Hamiltonian. We identify these terms analytically. They can provoke large length scale effects, such as the formation of interfaces and depletion layers. We apply our theory to compute the reversible work to form a bubble in liquid water, as a function of the bubble radius. Comparison with molecular simulation results for the same function indicates that the theory is reasonably accurate. Importantly, simulating the large length scale field involves binary arithmetic only. It thus provides a computationally convenient scheme to incorporate explicit solvent dynamics and structure in simulation studies of large molecular assemblies.

DOI: 10.1103/PhysRevE.65.011201

PACS number(s): 61.20.Gy, 68.08.-p, 82.70.Uv, 87.15.Aa

I. INTRODUCTION

We have constructed a tractable model for describing density fluctuations in a cold liquid at both small and large length scales. The model allows us to analyze at a microscopic level the effects of solvated surfaces and large molecular assemblies, perhaps of biophysical relevance. This paper presents the model and demonstrates its tractability.

A cold liquid is a fluid that is well below the critical temperature. Water at ambient conditions is an example. When unperturbed, it will have no significant large length scale fluctuations. It is nearly incompressible. When perturbed by a sufficiently extended surface, however, a cold liquid may exhibit large length scale fluctuations, akin to a phase transition, in the vicinity of the surface. This phenomenon occurs when another phase is close to coexistence with the liquid, and when interactions with the surface favors the other phase over the liquid. This coincidence of conditions is pertinent, for instance, to hydrophobic effects. In particular, water at ambient conditions lies close to coexistence with its vapor. Further, the demixing of oil and water and the associated large oil-water surface tension indicates that a large hydrophobic (i.e., oily) surface favors vapor over liquid water.

Indeed, Lum, Chandler, and Weeks (LCW) [1] have demonstrated that oily surfaces extending over 1 nm or more will nucleate a layer of depleted water density and concomitant large length scale correlations. In contrast, perturbations from smaller hydrophobic surfaces, less than 1 nm across, do not nucleate such a drying layer and affect only small length scale fluctuations in the liquid. Since hydrophobicity vividly manifests the interplay and competition between small and large length scale fluctuations in a cold liquid, we have chosen in this paper to focus attention on it. One benefit of our analysis is an understanding of the results of LCW theory from a perspective that is numerically simpler and physically more transparent than the original LCW development. Generalizations of our approach to other phenomena, including

the effects of strong associative interactions between solutes and solvent, should be apparent.

The main idea of our approach is to create a statistical field theory where the molecular density field is decomposed into two parts. One part varies on large length scales only. The other varies on small length scales. For a cold fluid that is homogeneous and therefore nearly incompressible, the large length scale field is nearly constant and equal to the mean density of the bulk liquid. Even for this homogeneous case, however, small length scale fluctuations are always present. To a remarkable extent [2,3], the statistics of these fluctuations is Gaussian with a variance determined by the structure factor of the bulk liquid. Accurate molecular theories of solvation and liquid structure at small length scales—the Percus-Yevick equation for hard-sphere fluids [4,5], the mean spherical approximation [6,7], the Pratt-Chandler theory of hydrophobicity [8], and the reference interaction site model [9,10]—are all consequences of such statistics [11]. These Gaussian statistics for small length scale fluctuations are an important element of the weight functional (or Hamiltonian) we construct. These fluctuations are coupled, of course, to the large length scale density field, and they are also constrained by the presence of solutes. Due to the coupling and constraints, the variance of the small length scale fluctuations may differ markedly from that of the homogeneous bulk fluid.

The Hamiltonian for our model is presented in Sec. II. The large length scale density field supports possible phase coexistence and interfaces. As such, we see in that section how the coupling between small and large length scale fields may lead to solute-induced interfaces in a cold fluid. Our treatment of this coupling is inspired by the work of Lum *et al.* and Weeks and his coworkers [1,12]. They related the coupling to unbalanced attractive forces that result from local inhomogeneities in the fluid. Analytical integration over the small length scale field is possible due to its Gaussian statistics. The integration yields an effective Hamiltonian

functional for the large length scale field. In Sec. III, we describe how this integration may be used to study solvation. This step also lays the foundation for a numerical scheme where the solvent is simulated at the level of the large length scale density field. Such a scheme involves only binary arithmetic and is much more efficient than an atomic level simulation. In fact, it is sufficiently efficient to make possible the study of phenomena like self-assembly of biological structures.

In Sec. IV, we discuss the results of our treatment in various limits. In the absence of any solutes, the effective Hamiltonian for the large length scale density corresponds to the lattice-gas model [13]. In the presence of solutes that are small in size and number, only those density fluctuations at small length scales are relevant, and our model reduces to the Gaussian model of Pratt and Chandler [8], and the closely related information theory approach of Hummer and coworkers [2]. In the presence of large solutes, a mean-field approximation to our model coincides with the LCW theory [1].

A numerical application is given in Sec. V. We first show how the parameters in our model may be estimated from experimentally accessible quantities. We then explicitly treat the solvation of an ideal hydrophobic sphere in water and compare our results with those of an atomistic simulation [14]. Finally, in Sec. VI, we discuss implications and possible extensions of this paper.

II. MODEL

Figure 1 illustrates the essential features of a cold fluid in the presence of a solute. The solute is of arbitrary size and shape. If it is small, the solvent will wet its surface. In contrast, if the solute is large with extended hydrophobic surfaces, solvent density near the solute will be depleted relative to the density of the bulk liquid ρ_l . This dryinglike phenomenon occurs because the solvent experiences unbalanced attractive forces near the hydrophobic surface. These forces induce depletion. The solute may also have patches of associative interactions. Adjacent to those patches, the molecular density of the solvent will be close to or perhaps greater than that of the bulk liquid.

In our description of solvation, we make a distinction between strong forces and weak solvent-solute forces. The repulsive nearly hard-core interactions between solute and solvent molecules are strong forces. So too are associative interactions between solute and solvent. On the other hand, dispersion interactions between solute and solvent molecules are weak forces. In some cases, electrostatic forces are weak forces. Weak interactions are described in our treatment by an interaction potential acting between the solute and the solvent density. In contrast, strong forces are treated according to the constraints they impose upon the solvent density fluctuations. For example, the effect of a solute repulsive core is mainly to exclude solvent from a volume v_{ex} in Fig. 1. The effect of these forces may be described as a constraint permitting only those fluctuations in the solvent density, $\rho(\mathbf{r})$, that leave v_{ex} empty of solvent, i.e., $\rho(\mathbf{r})=0$ for $\mathbf{r} \in v_{ex}$ [11]. Similarly, associative interactions may cause n water molecules to be bound within a specific region close to

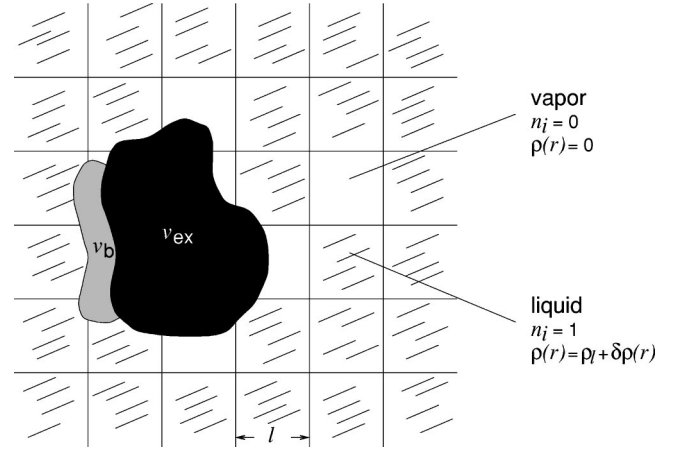


FIG. 1. Sketch of our model of a cold liquid in the presence of a solute. The solute excludes a volume v_{ex} from the solvent (black region) and has a hydrophilic patch of strong associative interactions with the solvent; the patch imposes a constraint on the solvent density in the volume v_b (gray area). The solvent is divided into cells of width l ; each cell is either filled with liquid ($n_i=1$) or vapor ($n_i=0$). The field n_i describes density fluctuations on length scales larger than the lattice spacing. This field supports phase transitions. Density fluctuations on length scales smaller than the lattice spacing are described by the field $\delta\rho(\mathbf{r})$. This field describes molecular detail such as the highly oscillatory profiles for the average density near small solutes. We thus write the density as $\rho(\mathbf{r}_i) = n_i\rho_l + \delta\rho(\mathbf{r}_i)$. The field $\delta\rho(\mathbf{r})$ is assumed to obey Gaussian statistics.

the solute. In Fig. 1, this region is v_b . This effect may be treated by constraining the integral of $\rho(\mathbf{r})$ over the volume v_b to equal n [1]. We do not apply this latter idea in the current paper, although the methods by which it may be implemented should be clear from our treatment of the former.

Since the fluid is assumed to be cold, the regions of gas or vapor may be clearly distinguished from those of liquid. The density of the vapor is typically orders of magnitude smaller than that of the liquid. In such a situation, it is natural to divide space into a grid of cells, where each cell contains either gas or liquid. We use cubic cells, and take the distance across each cell l to be comparable to the bulk liquid correlation length ξ . In that case, a binary choice of states within a cell, either gas or liquid, provides a reasonable coarse-grained rendering of likely configurations of the fluid. We can thus define a field n_i that takes on the value of one if cell i contains liquid and zero if it contains gas. The molecular density we associate with this field is $n_i\rho_l$. This field n_i or equivalently $n_i\rho_l$, is the large length scale field in our model. It may be used together with a second field $\delta\rho(\mathbf{r})$ to describe the density on length scales both larger and smaller than l . In particular, for positions \mathbf{r} within cell i , \mathbf{r}_i , we write the net density as

$$\rho(\mathbf{r}_i) = n_i\rho_l + \delta\rho(\mathbf{r}_i). \quad (1)$$

All of space is spanned by the set of \mathbf{r}_i , i.e., $\int d\mathbf{r} \equiv \sum_i \int d\mathbf{r}_i$.

While the field n_i is binary and may be used to describe a liquid-gas phase transition, the field $\delta\rho(\mathbf{r})$ has a very different character. It supports neither phase transitions nor interfaces, but it does describe small length scale structures, such as those manifesting the granularity of the solvent (e.g., the oscillatory profiles of the average liquid density in the vicinity of a small solute). It must be possible, therefore, that $\delta\rho(\mathbf{r})$ may take on a variety of values. As indicated in the Introduction, it is a reasonable approximation to adopt the simplest possible statistics for this field. Namely, we assume it is Gaussian and define its variance to be

$$\chi[\mathbf{r}_i, \mathbf{r}'_j; \{n_k\}] = \langle \delta\rho(\mathbf{r}_i) \delta\rho(\mathbf{r}'_j) \rangle_{\{n_k\}}. \quad (2)$$

Here, $\langle \cdot \cdot \rangle_{\{n_k\}}$ indicates the ensemble average over density fluctuations for a given configuration of the field n_k . The dependence upon n_k is significant. When $n_k=1$ for all k , corresponding to a cold liquid with absolutely no large length scale fluctuations, $\delta\rho(\mathbf{r}_i)$ has zero mean, and its variance reduces to the response function of the bulk fluid,

$$\chi(\mathbf{r}_i, \mathbf{r}'_j; \rho_l) = \rho_l \delta(\mathbf{r}_i - \mathbf{r}'_j) + \rho_l^2 h(|\mathbf{r}_i - \mathbf{r}'_j|; \rho_l), \quad (3)$$

where $h(|\mathbf{r}_i - \mathbf{r}'_j|; \rho_l) + 1$ is the radial distribution function of the uniform fluid at density ρ_l . On the other hand, within a cell that contains vapor ($n_i=0$), small length scale fluctuations are very small. Our model employs the approximation that $\delta\rho(\mathbf{r}_i)=0$ whenever $n_i=0$. Therefore, we imagine that $\delta\rho(\mathbf{r})$ is a Gaussian field, with a weight functional being that of the bulk fluid, but constrained to be zero whenever $n_i=0$. The response function for such a field is [11]

$$\begin{aligned} \chi[\mathbf{r}_i, \mathbf{r}'_j; \{n_k\}] &= \chi(\mathbf{r}_i, \mathbf{r}'_j; \rho_l) \\ &- \sum_k \sum_l \int d\mathbf{r}''_k \int d\mathbf{r}'''_l \chi(\mathbf{r}_i, \mathbf{r}''_k; \rho_l) \\ &\times \chi_g^{-1}[\mathbf{r}''_k, \mathbf{r}'''_l; \{n_k\}] \chi(\mathbf{r}'''_l, \mathbf{r}'_j; \rho_l). \end{aligned} \quad (4)$$

Here,

$$\begin{aligned} \chi_g[\mathbf{r}_i, \mathbf{r}'_j; \{n_k\}] &= \chi(\mathbf{r}_i, \mathbf{r}'_j; \rho_l) \quad \text{if } n_i = n_j = 0, \\ &= 0, \quad \text{otherwise,} \end{aligned} \quad (5)$$

is the $(\mathbf{r}_i, \mathbf{r}'_j)$ element of the matrix χ_g . Similarly, the matrix with elements $\chi_g^{-1}[\mathbf{r}_i, \mathbf{r}'_j; \{n_k\}]$ is also nonzero only when $n_i = n_j = 0$. In that space, where $n_i = 0$, χ_g^{-1} is the inverse of χ_g . These relations project the matrix with elements $\chi_g^{-1}[\mathbf{r}_i, \mathbf{r}'_j; \{n_k\}]$ onto the space of cells for which $n_i = 1$. We adopt these relations to define our model of Gaussian statistics for $\delta\rho(\mathbf{r})$.

With the lattice spacing as large as the bulk correlation length, the field $n_i \rho_l$ is nearly incompressible. This means that in the absence of any strong perturbations on the fluid, the field n_i is essentially constant. In this case of the unperturbed (i.e., uniform) fluid, density fluctuations are described almost entirely by the field $\delta\rho(\mathbf{r})$. The compressibility of the uniform fluid is contained in the variance for $\delta\rho(\mathbf{r})$. In this context, consider the behavior of the bulk liquid structure

factor, $\int d(\mathbf{r} - \mathbf{r}') \chi(\mathbf{r}, \mathbf{r}'; \rho_l) \exp[i\mathbf{k} \cdot (\mathbf{r} - \mathbf{r}')]]$. The long-wave length limit of the structure factor is proportional to the bulk compressibility. It approaches this limit with a plateau. In particular, for k values smaller than some finite wave-vector k_c , the structure factor is essentially constant. The grid spacing we use to define large length scales coincides with $l \sim 2\pi/k_c$.

To within a physically irrelevant metric factor, the partition function for our model is

$$\begin{aligned} \Xi &= \sum_{\{n_i\}} \int \mathcal{D}\delta\rho(\mathbf{r}) C[\{n_k\}, \delta\rho(\mathbf{r})] \\ &\times \exp(-\beta H[\{n_k\}, \delta\rho(\mathbf{r})]), \end{aligned} \quad (6)$$

where $\int \mathcal{D}\delta\rho(\mathbf{r}) = \int \prod_i \mathcal{D}\delta\rho(\mathbf{r}_i)$ denotes the functional integration over the small length scale field, $H[\{n_k\}, \delta\rho(\mathbf{r})]$ is the Hamiltonian as a functional of both n_i and $\delta\rho(\mathbf{r})$, and β^{-1} is Boltzmann's constant time temperature $k_B T$. The quantity $C[\{n_k\}, \delta\rho(\mathbf{r})]$ is a constraint functional. It has unit weight when the field $\delta\rho(\mathbf{r})$, together with $\{n_i\}$, satisfy whatever constraints are imposed by strong forces, and it is zero otherwise. Since $\{n_i\}$ and $\delta\rho(\mathbf{r})$ have a greatly different character, the summation and integration in Eq. (6) do not redundantly count configuration space to any significant degree.

In our model, there are three principal contributions to the Hamiltonian, $H[\{n_k\}, \delta\rho(\mathbf{r})]$. One is a lattice-gas Hamiltonian for the large length scale field,

$$H_L[\{n_k\}] = -\mu \sum_i n_i - \epsilon \sum_{\langle i,j \rangle} n_i n_j. \quad (7)$$

Here, μ is the imposed chemical potential, the sum labeled with $\langle i,j \rangle$ is over all nearest-neighbor pairs of cells, and the interaction parameter ϵ determines the energetic cost of creating a vapor-liquid interface. Importantly, the lattice-gas model supports phase transitions and sustains gas-liquid interfaces.

A second contribution to the Hamiltonian ensures the Gaussian weight for the small length scale field. From the principle of equipartition, this contribution must be

$$\frac{k_B T}{2} \sum_{i,j} \int d\mathbf{r}_i \int d\mathbf{r}'_j \delta\rho(\mathbf{r}_i) \chi^{-1}[\mathbf{r}_i, \mathbf{r}'_j; \{n_k\}] \delta\rho(\mathbf{r}'_j). \quad (8)$$

A third contribution to the Hamiltonian gives the coupling between the n_i and $\delta\rho(\mathbf{r})$ fields arising from unbalanced forces. According to the arguments provided by Lum *et al.* and Weeks and coworkers for simple fluids [1,12], the unbalancing potential acting on n_i for a simple fluid is well estimated by $-2a\langle \delta\rho(\mathbf{r}) \rangle$. Here, $a\rho_l^2$ is the energy density of the uniform liquid at density ρ_l , and the overbar denotes a coarse graining of the density fluctuation $\delta\rho(\mathbf{r})$ over a length scale comparable to the bulk correlation length. Based upon this estimate, we write the contribution to the Hamiltonian from unbalanced forces as

$$-\epsilon' \sum_{i,j(\text{nni})} \int d\mathbf{r}_i \delta\rho(\mathbf{r}_i) \frac{n_j-1}{\rho l^3}, \quad (9)$$

for simple fluids with only one energy and length scale $\epsilon' = \epsilon$. This equality implies that the lattice-gas parameters ϵ and l are sufficient to determine both the surface tension and the energy density of the liquid. For more complex fluids, including water, the effects of orientational degrees of freedom may introduce multiple microscopic length scales, and as a result, ϵ' could differ from ϵ . This possibility was ignored in Ref. [1], but will be examined in Sec. VI.

By combining all three contributions, we arrive at our final result for the Hamiltonian of our model. It is

$$\begin{aligned} H[\{n_k\}, \delta\rho(\mathbf{r})] &= H_L[\{n_k\}] - \epsilon' \sum_{i,j(\text{nni})} \int d\mathbf{r}_i \delta\rho(\mathbf{r}_i) \frac{n_j-1}{\rho l^3} \\ &+ \frac{k_B T}{2} \sum_{i,j} \int d\mathbf{r}_i \int d\mathbf{r}'_j \\ &\times \delta\rho(\mathbf{r}_i) \chi^{-1}[\mathbf{r}_i, \mathbf{r}'_j; \{n_k\}] \delta\rho(\mathbf{r}'_j) \\ &+ H_{\text{norm}}[\{n_k\}], \end{aligned} \quad (10)$$

where

$$\begin{aligned} H_{\text{norm}}[\{n_k\}] &= \frac{k_B T}{2} \sum_{i,k(\text{nni})} \sum_{j,l(\text{nnj})} \int d\mathbf{r}_i \int d\mathbf{r}'_j \\ &\times \phi_k \chi[\mathbf{r}_i, \mathbf{r}'_j; \{n_k\}] \phi_l + k_B T \ln \sqrt{\det \chi}, \end{aligned} \quad (11)$$

and

$$\phi_j = \beta \epsilon' \frac{n_j-1}{\rho l^3}. \quad (12)$$

Here, the quantity $\det \chi$ is the determinant of the matrix with elements $\chi[\mathbf{r}_i, \mathbf{r}'_j; \{n_k\}]$. The last term in Eq. (10), $H_{\text{norm}}[\{n_k\}]$, provides a normalization constant for the functional integration over $\delta\rho(\mathbf{r})$. When there are no strong forces, so that the constraint functional $C[\{n_k\}, \delta\rho(\mathbf{r})]$ is simply unity, the effective Hamiltonian for the n_i field should be exactly the lattice-gas Hamiltonian, Eq. (7). The last term in Eq. (10) ensures that the integration over $\delta\rho(\mathbf{r})$ for this case will indeed yield this result.

III. THEORY OF SOLVATION

The excess chemical potential of a solute $\Delta\mu$ is given by [15]

$$\beta\Delta\mu = -\ln \frac{\Xi_S}{\Xi} = -\ln \langle \exp(-\beta U_S) \rangle_0. \quad (13)$$

Here, Ξ is the partition function for the unperturbed solvent and Ξ_S is the partition function for the system in the presence of a (fixed) solute. The energy U_S is the energy of

interaction between the solute and the solvent molecules and the subscript 0 denotes an ensemble average over the unperturbed solvent.

For simplicity, we will consider the solvation of an ideal hydrophobic solute in water—a particle that excludes water from a region v_{ex} , but has no other interactions with the solvent. A hard sphere is an example of an ideal hydrophobic solute. It excludes solvent from a volume $v_{\text{ex}} = (4/3)\pi R^3$, where the radius R is the distance of closest approach between water and solute. The partition function of the system in the presence of such a solute is equal to the partition function of the unperturbed solvent, but with the constraint that no solvent exists inside the excluded volume. In other words, the constraint functional for this case is

$$C[\{n_k\}, \delta\rho(\mathbf{r})] = \prod_{\mathbf{r}_i \in v_{\text{ex}}} \delta[n_i \rho_l + \delta\rho(\mathbf{r}_i)]. \quad (14)$$

Accordingly, the partition function in the presence of an ideal hydrophobic solute is

$$\begin{aligned} \Xi_S &= \sum_{\{n_i\}} \int \prod_i \mathcal{D}\delta\rho(\mathbf{r}_i) \left\{ \prod_{\mathbf{r}_i \in v_{\text{ex}}} \delta[n_i \rho_l + \delta\rho(\mathbf{r}_i)] \right\} \\ &\times \exp(-\beta H[\{n_k\}, \delta\rho(\mathbf{r})]). \end{aligned} \quad (15)$$

For an ideal hydrophobic solute, the ratio of partition functions Ξ_S/Ξ equals the probability of observing no solvent molecules inside the volume v_{ex} . Equivalently, it corresponds to the probability of observing a cavity of volume v_{ex} inside the solvent; it is also equal to the probability that a solute may be inserted into the solvent without creating any overlap with the solvent molecules. The excess chemical potential of an ideal solute could be obtained by imposing an alternative constraint,

$$C[\{n_k\}, \delta\rho(\mathbf{r})] = \delta \left[\int_{\mathbf{r} \in v_{\text{ex}}} d\mathbf{r} \rho(\mathbf{r}) \right]. \quad (16)$$

Were our treatment completely consistent with the particulate nature of matter, the two constraints, as given by Eqs. (14) and (16), would be equivalent. But in fact, Gaussian statistics for the field $\delta\rho(\mathbf{r})$ cannot be completely consistent with this nature of matter, and the two constraint functionals will yield somewhat different results.

To evaluate the partition function Eq. (15), it is convenient to rewrite the constraint functional with the Fourier representation of delta functions. Namely,

$$\begin{aligned} \Xi_S &= \sum_{\{n_i\}} \int \prod_i \mathcal{D}\delta\rho(\mathbf{r}_i) \int \prod_i \mathcal{D}\psi(\mathbf{r}_i) \\ &\times \exp \left(-\beta H[\{n_k\}, \delta\rho(\mathbf{r})] \right. \\ &\left. + i \sum_i \int_{\mathbf{r}_i \in v_{\text{ex}}} d\mathbf{r}_i \psi(\mathbf{r}_i) [n_i \rho_l + \delta\rho(\mathbf{r}_i)] \right). \end{aligned} \quad (17)$$

Functional integration over both $\delta\rho(\mathbf{r})$ and $\psi(\mathbf{r})$ is now straightforward, yielding

$$\Xi_S = \sum_{\{n_i\}} \exp(-\beta H[\{n_k\}]), \quad (18)$$

where the effective Hamiltonian $H[\{n_k\}]$ is

$$\begin{aligned} H[\{n_k\}] = & H_L[\{n_k\}] + \frac{k_B T}{2} \sum_{i,j} \int_{\mathbf{r}_i \in v_{\text{ex}}} d\mathbf{r}_i \int_{\mathbf{r}'_j \in v_{\text{ex}}} d\mathbf{r}'_j \\ & \times [n_i \rho_l + f(\mathbf{r}_i)] \chi_{\text{in}}^{-1}[\mathbf{r}_i, \mathbf{r}'_j; \{n_k\}] [n_j \rho_l + f(\mathbf{r}'_j)] \\ & + k_B T \ln \sqrt{\det \chi_{\text{in}}}, \end{aligned} \quad (19)$$

with

$$f(\mathbf{r}_i) \equiv \beta \epsilon' \sum_j \int d\mathbf{r}'_j \sum_{k(\text{nnj})} \frac{n_k - 1}{\rho_l l^3} \chi[\mathbf{r}_i, \mathbf{r}'_j; \{n_k\}]. \quad (20)$$

Here, χ_{in} has elements $\chi[\mathbf{r}_i, \mathbf{r}'_j; \{n_k\}]$ for \mathbf{r}_i and \mathbf{r}'_j both within the excluded volume, and a sum over $k(\text{nnj})$ is over cells k that are nearest neighbors to cell j .

The evaluation of $H[\{n_k\}]$ requires the calculation of various integrals and matrix inverses. These quantities can be conveniently estimated to a good approximation by exploiting the fact that the lattice spacing is on the order of the bulk correlation length. In particular, since the bulk correlation function, $\chi(\mathbf{r}_i, \mathbf{r}'_j; \rho_l)$ vanishes quickly for $|\mathbf{r} - \mathbf{r}'|$ larger than that length, $\chi[\mathbf{r}_i, \mathbf{r}'_j; \{n_k\}]$ as given by Eq. (4), may be approximated by

$$\begin{aligned} \chi[\mathbf{r}_i, \mathbf{r}'_j; \{n_k\}] &= \chi(\mathbf{r}_i, \mathbf{r}'_j; \rho_l), \quad \text{for } n_i = n_j = 1 \\ &= 0, \quad \text{otherwise.} \end{aligned} \quad (21)$$

Furthermore, the relatively large size of the cells allows us to restrict the sum in Eq. (20) to the $i=j$ term, and to take the integral over all space, rather than over one cell. As such, we arrive at a much simplified form for $f(\mathbf{r}_i)$, and therefore,

$$f_i \equiv \int_{\mathbf{r}_i \in v_{\text{ex}}} d\mathbf{r}_i f(\mathbf{r}_i) = n_i v_i \epsilon' \kappa \frac{\rho_l}{l^3} \sum_{k(\text{nni})} (n_k - 1). \quad (22)$$

Here, κ is the isothermal compressibility of the uniform fluid, which is related to the response function via $\kappa = \beta \hat{\chi}(0) / \rho_l^2$, where $\hat{\chi}(0)$ is the long-wave length limit of the Fourier transform of the structure factor. Note that f_i is zero, when cell i is not liquid, i.e., when $n_i = 0$.

Finally, with $\chi(\mathbf{r}_i, \mathbf{r}'_j; \rho_l)$ provided as input into the theory, we must choose a set of basis functions that span the space of the excluded manifold. This allows us to perform the inversion of $\chi_{\text{in}}[\mathbf{r}_i, \mathbf{r}'_j; \{n_k\}]$ in the representation prescribed by that basis. We use the approximation of a one-basis function spanning the excluded volume and to take $\chi_{\text{in}}[\mathbf{r}_i, \mathbf{r}'_j; \{n_k\}] = \chi(\mathbf{r}_i, \mathbf{r}'_j; \rho_l)$ for all cells i inside the excluded volume [16]. We then arrive at our principal result

$$\begin{aligned} H[\{n_k\}] &= H_L[\{n_k\}] + k_B T \sum_{i,j(\text{occ})} \frac{n_i [\rho_l v_i + f_i] [\rho_l v_j + f_j] n_j}{2 \sigma_{v_{\text{ex}}}} \\ &+ k_B T \ln \sqrt{2 \pi \sigma_{v_{\text{ex}}}}; \\ &\equiv H_L[\{n_k\}] + H_S[v_{\text{ex}}; \{n_k\}]. \end{aligned} \quad (23)$$

Here, the sum over $i, j(\text{occ})$ is over cells i and j that are occupied by the solute; v_i is the volume occupied by the solute in cell i , and

$$\sigma_{v_{\text{ex}}} = \int_{v_{\text{ex}}} d\mathbf{r} \int_{v_{\text{ex}}} d\mathbf{r}' \chi(\mathbf{r}, \mathbf{r}'; \rho_l). \quad (24)$$

In the one-basis set approximation for $\chi[\mathbf{r}_i, \mathbf{r}'_j; \{n_k\}]$, employed to arrive at Eq. (23), the effect of the constraint functional as given by Eq. (14) reduces to that of the constraint functional as given by Eq. (16).

The term $H_S[v_{\text{ex}}; \{n_k\}]$ contains all the effects of the interaction between the solute and the ideal hydrophobic solvent. It increases with increasing solute size, if $n_i = 1$ for the cells i that are occupied by the solute. The interaction term solely arises from the constraint that is imposed on the allowed density fluctuations of the solvent. This idea, that solvation of a hydrophobic species is equivalent to the effect of imposing a constraint on the solvent density, is an important feature of our model. Interestingly, the excess chemical potential of the solute may be obtained by averaging this interaction free energy as follows:

$$\begin{aligned} \beta \Delta \mu(v_{\text{ex}}) &= -\ln \frac{\Xi_S}{\Xi} \\ &= -\ln \frac{\sum_{\{n_i\}} \exp(-\beta H[\{n_k\}])}{\sum_{\{n_i\}} \exp(-\beta H_L[\{n_k\}])} \\ &= -\ln \langle \exp(-\beta H_S[v_{\text{ex}}; \{n_k\}]) \rangle_L, \end{aligned} \quad (25)$$

where $\langle \dots \rangle_L$ indicates the ensemble average with the Hamiltonian $H_L[\{n_k\}] = H[\{n_k\}] - H_S[v_{\text{ex}}; \{n_k\}]$.

The simple formula for $H[\{n_k\}]$, Eq. (23), and similar formulas for more general cases, may be of enormous practical benefit for studying self assembly. Such studies usually require large system sizes. In those cases, the treatment of solvent is a primary computational bottleneck. This is because large solutes are solvated by a huge number of solvent molecules, and an atomistic treatment involves a correspondingly large number of coordinates and momenta. The formula for $H[\{n_k\}]$, however, lays the foundation for a scheme in which only the solutes are treated explicitly at the atomic level; the solutes may be moved by a continuous Monte Carlo or molecular-dynamics scheme. The solvent, on the other hand, is simulated in terms of the large length scale density field n_i . That field may be propagated by a dynamic

Monte Carlo procedure, manipulating only binary numbers. More details of this scheme will be discussed in a forthcoming publication [17].

IV. LIMITING RESULTS AND COMPARISONS WITH OTHER THEORIES

Consider first the case where $n_i=1$ for all i . This case is physically pertinent for solutes small in size and in number because the concomitantly small value of v_{ex} leads to relatively small free energetic costs for having $n_i=1$ for all cells i , even for the cells that are occupied by the solute. Specifically, when the solutes occupy relatively small volumes, the amount that $H_S[v_{\text{ex}}; \{n_k\}]$ will decrease by changing n_i from 1 to 0 will not compensate the corresponding increase in $H_L[\{n_k\}]$. With $n_i=1$ for all i , $H_L[n]$ and $H_{\text{norm}}[\{n_i\}]$ become constants and thus irrelevant. The response function $\chi[\mathbf{r}_i, \mathbf{r}'_j; \{n_k\}]$ reduces to the response function of the uniform fluid $\chi(\mathbf{r}, \mathbf{r}'; \rho_l)$. Further, the coupling term in Eq. (10) becomes identically zero. As such, the Hamiltonian for the model reduces to that of the Gaussian model of Pratt and Chandler [8,11], namely, $H[\{n_i\}, \delta\rho(\mathbf{r})] \rightarrow H_G[\delta\rho(\mathbf{r})]$, where

$$H_G[\delta\rho(\mathbf{r})] = \frac{k_B T}{2} \int d\mathbf{r} \int d\mathbf{r}' \delta\rho(\mathbf{r}) \chi^{-1}(\mathbf{r}, \mathbf{r}'; \rho_l) \delta\rho(\mathbf{r}'), \quad (26)$$

with $\delta\rho(\mathbf{r}) = \rho(\mathbf{r}) - \rho_l$, and the response function $\chi^{-1}(\mathbf{r}, \mathbf{r}'; \rho_l)$ being the response function of the uniform fluid. Similarly, applying Eq. (25), we obtain the excess chemical potential for the ideal hydrophobic solute: $\beta\Delta\mu(v_{\text{ex}}) = -\ln(\exp(-\beta H_S[v_{\text{ex}}; \{1\}]))_L = \beta H_S[v_{\text{ex}}; \{1\}]$. But, if $n_i=1$ for all i , then $f_i=0$ for all i , and so

$$\beta\Delta\mu(v_{\text{ex}}) \approx \rho_l^2 v_{\text{ex}}^2 / 2\sigma_{v_{\text{ex}}} + \ln\sqrt{2\pi\sigma_{v_{\text{ex}}}}. \quad (27)$$

For excluded volumes not unphysically small, this formula for the excess chemical potential is the solvation energy result of Hummer and Pratt and their coworkers [2,18]. We see that it is the result of Gaussian statistics in the one-basis set approximation.

In contrast to setting $n_i=1$ for all i , the treatment of LCW [1] assumes that n_i can be replaced by $\langle n_i \rangle$, where $\langle n_i \rangle$ is an estimate of the mean value of n_i . In that case, Eq. (25) gives

$$\begin{aligned} \beta\Delta\mu(v_{\text{ex}}) &\approx H_L[\{\langle n_k \rangle\}] - H_L[\{1\}] + \beta H_S[v_{\text{ex}}; \{\langle n_k \rangle\}] \\ &\approx H_L[\{\langle n_k \rangle\}] - H_L[\{1\}] \\ &\quad + k_B T \sum_{i,j(\text{occ})} \langle n_i \rangle \langle n_j \rangle \rho_l^2 v_i v_j / 2\sigma_{v_{\text{ex}}} \\ &\quad + k_B T \ln\sqrt{2\pi\sigma_{v_{\text{ex}}}}, \end{aligned} \quad (28)$$

where the second approximate equality follows from the first after neglecting f_i and f_j in comparison with $v_i \rho_l$ and $v_j \rho_l$, respectively. Except in the crossover regime, this is usually a reasonable approximation, because $\kappa \rho_l / \beta \sim 10^{-2}$. Within

notational differences, Eq. (28) is the solvation energy result given by LCW theory, Eq. (9) of Ref. [1].

The LCW formula for the mean large length scale field, $\langle n_i \rangle$, may also be understood from our model. In particular, in Eq. (10), let us replace in the second term the field $\delta\rho(\mathbf{r}_i)$ with its mean, $\langle \delta\rho(\mathbf{r}_i) \rangle$. With this replacement, the first two terms in Eq. (10) give the mean molecular field ϕ_j acting on n_j

$$\begin{aligned} \phi_j &= -\mu - \sum_{i(\text{nn}j)} \left[\epsilon \langle n_i \rangle + \epsilon' \int d\mathbf{r}_i \langle \delta\rho(\mathbf{r}_i) \rangle / \rho_l l^3 \right] \\ &\approx -\mu - \epsilon \sum_{i(\text{nn}j)} [\langle n_i \rangle + \overline{\langle \delta\rho(\mathbf{r}_i) \rangle} / \rho_l], \end{aligned} \quad (29)$$

where the approximate equality follows principally from approximating ϵ' with ϵ . For the coarse graining indicated by the over bar, we use l as the coarse-graining length. Other contributions to the mean molecular field come from the quadratic term in $\delta\rho(\mathbf{r})$ and from H_{norm} . These, however, are small outside the crossover regime, either because they appear in the logarithm or because they arise from unlikely configurations, where one neighboring cell is filled while another is empty. With the molecular field in Eq. (29), the LCW self-consistent equation for $\langle n_j \rangle$ is obtained. Specifically, since both $\langle n_i \rangle$ and $\langle \delta\rho(\mathbf{r}_i) \rangle / \rho_l$ vary slowly in space, they may be expanded for i close to j about $\langle n_j \rangle$ and $\overline{\langle \delta\rho(\mathbf{r}_i) \rangle} / \rho_l$, respectively. Truncating the expansion of $\langle n_i \rangle$ at the square gradient order, and the expansion for $\langle \delta\rho(\mathbf{r}_i) \rangle / \rho_l$ at lowest order, Eq. (29) gives Eq. (5) of Ref. [1]. Thus, the principal results of LCW may be understood as a mean-field approximation to the model we have presented herein.

V. APPLICATION TO HYDROPHOBIC SOLVATION: FREE ENERGY TO HYDRATE A SPHERICAL BUBBLE

A. Parameters

To apply our model, experimentally accessible quantities such as the structure factor and the surface tension of the solvent must be known. For the structure factor, we use the data of Narten and Levy for water [19]. For the energy parameter ϵ , we consider its connection to the experimental vapor-liquid surface tension of water, γ . Namely, since the liquid is cold, we use the low-temperature relation,

$$\gamma = \frac{\epsilon}{2l^2}. \quad (30)$$

Since the lattice spacing l should be on the order of the bulk correlation length, ξ , we have chosen $\xi \approx l = 4.2 \text{ \AA}$. We have verified that the results, such as those given below, do not depend strongly on the precise value of the lattice spacing by varying it between $l = 3.5 \text{ \AA}$ and $l = 5.0 \text{ \AA}$. With $\gamma = 70 \text{ mN/m}$, this yields $\epsilon = 6.02 k_B T$.

For a rough estimate of the energy parameter ϵ' , we consider its approximate connection with the energy density of the fluid, $-a\rho_l^2$. In particular,

$$a \approx \frac{z\epsilon'}{2\rho_l^2 l^3}, \quad (31)$$

where $z=6$ is the coordination number of the lattice of the cubic lattice-gas model. We arrive at this approximation by noting that a lattice-gas model with interaction energy parameter ϵ' will have an energy density $z\epsilon'/2l^3$. This estimate is strictly correct for a model with a single length and energy scale. We will see shortly that ϵ' obtained by applying Eq. (31) to water differs substantially from the ϵ as obtained by applying Eq. (30) to water. This difference is evidence of the fact that the microscopic nature of water is characterized by more than one length scale and perhaps by more than one energy scale. It is also evidence of the fact that Eq. (31) provides no better than a rough estimate of ϵ' . Nevertheless, it is worth evaluating that estimate, as it provides a value for this parameter that will be seen to be within 50% of the empirically correct value.

To apply Eq. (31), the energy density parameter a was derived from the internal energy U , which was obtained in the following way

$$U(298 \text{ K}) \approx \Delta H_{\text{vap}}(373 \text{ K}) + \int_{373}^{298} c_p dT, \quad (32)$$

where ΔH_{vap} is the heat of vaporization and c_p is the heat capacity. With $\Delta H_{\text{vap}} = -40.7 \text{ kJ/mol}$, $c_p = 75.3 \text{ J/K/mol}$, this yields $a = 566 \text{ k}_B T \text{ \AA}^3$, and thus, $\epsilon' \approx 15.2 \text{ k}_B T$. Thus, Eq. (31) estimates that ϵ' is nearly three times larger than ϵ . As such, it indicates that the unbalancing potential is strong enough to induce a vapor layer near the surface of a large hydrophobic object.

For the imposed chemical-potential μ we use

$$\mu = \mu_{\text{coex}} + \Delta\mu \approx \mu_{\text{coex}} + \Delta P l^3, \quad (33)$$

where $\mu_{\text{coex}} = -3\epsilon$ is the chemical potential at coexistence, and ΔP is the difference between the pressure at ambient conditions and the pressure at coexistence. With $\Delta P = 1.0 \times 10^5 \text{ Pa}$, the chemical-potential change is $\Delta\mu = 5.50 \times 10^{-4} \text{ k}_B T$. Note that $\Delta\mu$ is very small. Water at ambient conditions is indeed close to coexistence with its vapor.

B. Results

To test whether the theory successfully addresses density fluctuations at all length scales, a good benchmark is the excess chemical potential of an ideal solvophobic solute in a solvent as a function of its size [1,20,21]. Here, we present results for the solvation of a hard sphere (i.e., spherical bubble) in water.

The excess chemical-potential $\Delta\mu$ of a hard sphere that excludes solvent from a region of volume v_{ex} , is given by Eq. (25). We may obtain the excess chemical potential as a function of v_{ex} by sampling the size distribution of a “breathing” hard sphere with the Hamiltonian $H[\{n_k\}]$ shown in Eq. (23). Specifically, in a Monte Carlo trajectory for the large length scale field, each trial move consisted either of an attempt to flip a spin or to change the radius of

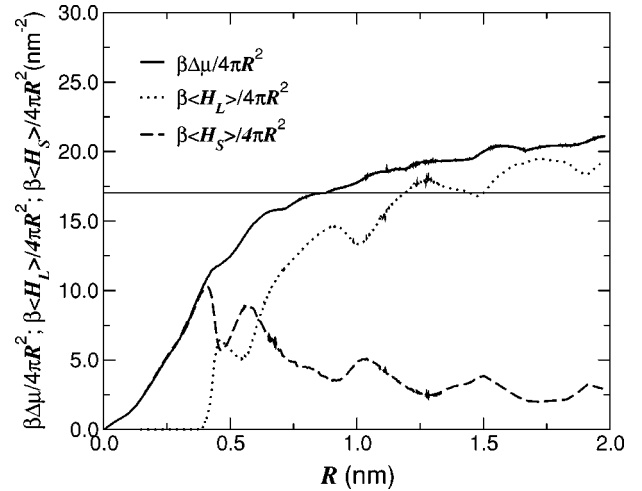


FIG. 2. The excess chemical potential per unit area of a hard sphere in water as a function of its size; the hard sphere excludes water from a spherical volume of radius R . The dotted line indicates the average potential energy from the bare lattice-gas model as given by $H_L[n]$ in Eq. (23) and the dashed line gives the average potential energy of the solute-solvent interaction as given by $H_S[n]$ in Eq. (23). It is seen that the lattice artifacts in the two-energy contributions tend to cancel each other. The horizontal line lies at the value of the surface tension γ of the vapor-liquid interface of water.

the solute; the trial moves are accepted with a probability proportional to $\exp(-\beta\Delta H)$, where ΔH is the change in $H[\{n_k\}]$ due to the move. In order to obtain accurate statistics for all solute sizes, we have used umbrella sampling [22].

Figure 2 shows the excess chemical potential of a hard sphere as a function of R , where R is the radius of the spherical excluding volume. The results do exhibit some lattice artifacts. These artifacts, however, are surprisingly small given the fact that the cells are quite large. The broken lines in Fig. 2 reveal why the lattice artifacts are small. These curves show the contribution to the solvation free energy from the energy of the solvent, as given by $H_L[\{n_k\}]$, and from the energy of the “solute-solvent” interaction, as given by $H_S[v_{\text{ex}}; \{n_k\}]$ in Eq. (23). Clearly, the discrete nature of our separation of length scales is manifest in the strong energy changes at intervals of length comparable to the grid spacing. This behavior is not surprising, as the large length scale field n_i is effectively very cold ($\epsilon = 6.02 \text{ k}_B T$). The important point to note is that the lattice artifacts in the respective free-energy contributions tend to properly cancel each other.

In Fig. 3, we compare the results of our model with the predictions of the Gaussian model Eq. (27) and with the results of a molecular simulation of a hard sphere in extended simple point charge (SPC/E) water [14]. It is seen that for small solute sizes, the agreement between the results of the fluid models and the SPC/E-simulation results is very good. The agreement is expected, since for small solutes, the large length scale density field remains close to its value in the unperturbed fluid with $\langle n_i \rangle \approx 1$, as can be seen from the radial density profiles in Fig. 4. In this regime, our model

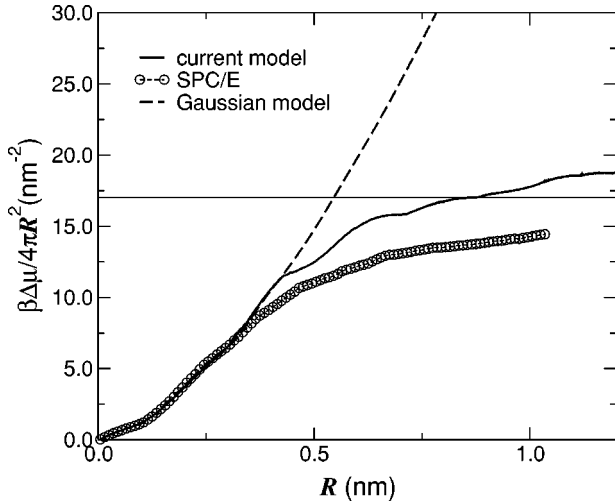


FIG. 3. Comparison of the results of the present model with the predictions of the Gaussian model Eq. (27) and the results of a molecular simulation of a cavity in SPC/E water [14]. The horizontal line lies at the value of the surface tension γ of the vapor-liquid interface of water.

reduces to the Gaussian model, Eq. (26). Computer simulations have shown that at small length scales, density fluctuations in water obey Gaussian statistics [2]. Thus, a Gaussian model, and hence the present model, successfully predict the excess chemical potential of small apolar species in water.

For solutes with $R > 4 \text{ \AA}$, the predictions of the Gaussian theory diverge from those of the full theory. The divergence is due to drying, as revealed in Fig. 4. The large length scale field $\langle n_i \rangle$ approaches a vaporlike value in the core of the larger solutes. Gaussian models cannot describe this drying or depletion, because they are based upon a density expan-

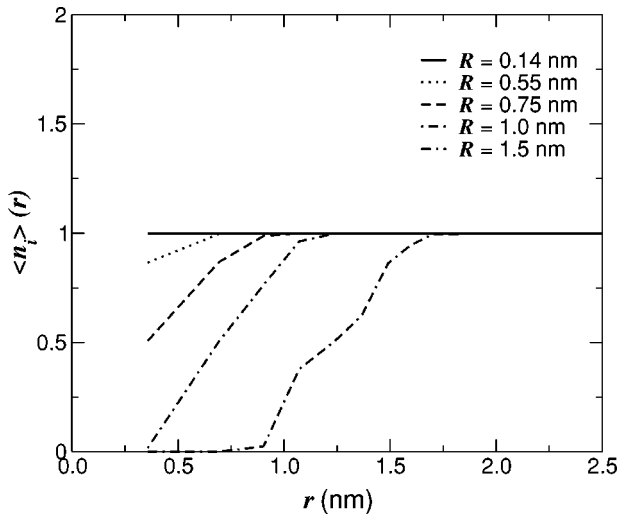


FIG. 4. Slowly varying density $\langle n(r) \rangle$ for hard spheres of different size, as a function of r , where r is the distance to the center of the solute. This radial profile was obtained by averaging n_i in concentric shells of radius r and width $\Delta r = 0.1 \text{ \AA}$. It is seen that the small solutes are in the wetting regime $\langle n(r) \rangle \approx \langle n(r) \rangle_o \approx 1.0$, whereas the larger solutes are in the drying regime, for which $\langle n(r) \rangle$ approaches a vaporlike value in the core of the solute.

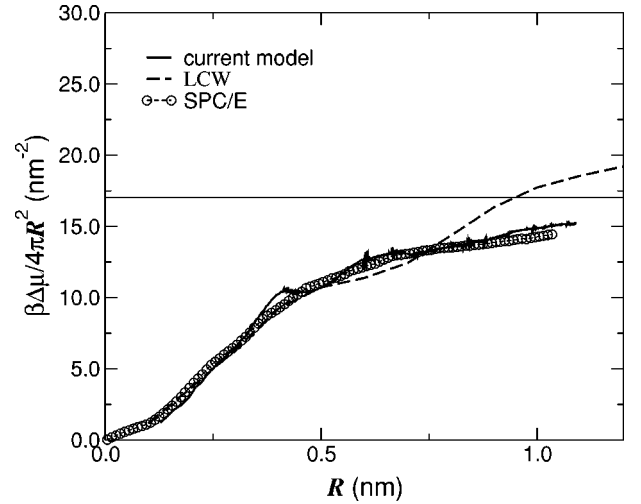


FIG. 5. Excess chemical potential per unit area for a hard sphere in water at ambient conditions (solid line). Here, the energy density a and the interaction parameter ϵ' are increased by 50% with respect to the results shown in Fig. 3. The dashed line denotes the results of the theory developed by Lum, Chandler, and Weeks [1]. The molecular simulation results for a cavity in SPC/E water are indicated by the circles [14].

sion around the uniform fluid. In order to describe drying, a fluid model has to support such a microscopic manifestation of a gas-liquid phase transition.

One of the attractive features of the present model is that it lays bare the relative contributions to the solvation free energy. In the crossover regime, the contribution to the Hamiltonian from the unbalancing potential, is very important. When we increase ϵ' by fifty percent from that estimated by Eq. (31), the results of the model agree very well with the simulation results over the entire range over which there is simulation data. In particular, compare Figs. 3 and 5. Evidently, orientational degrees of freedom result in an unbalancing potential that is larger than that estimated for simple fluids. With the simple fluid estimate of the unbalancing potential, the LCW theory [1] overestimates the excess chemical potential in the crossover regime. It appears that a somewhat larger unbalancing potential would correct this deficiency in LCW theory as it does in the current model.

It is often assumed that the excess chemical potential of an apolar species in water is proportional to its exposed surface area. Our results, as well as those of the LCW theory, emphasize that this is a reasonable assumption in the drying regime. As the solvent is near phase coexistence, the difference in chemical potential between vapor and liquid is small, and the work done to insert a solute predominantly arises from the work to create a vapor-liquid interface. For small solutes, however, the excess chemical potential does not scale in this way. To a better approximation, in this regime, it is a linear function of v_{ex} , as can be seen from Figs. 3 and 5.

VI. DISCUSSION

We have developed a model for a cold liquid that captures the effects of density fluctuations at both small and large length scales. This development is important, because many

phenomena in liquids involve the interplay of density fluctuations in the two regimes. One example is capillary condensation, another is hydrophobicity. Here, we have focused on the solvation of a hydrophobic species. Its nature is very different at small and large length scales. At small length scales, solvation is dominated by entropic effects. In this regime, the solvent may still wet the surface of the solute, even when the solute is highly hydrophobic [1,20]. In contrast, at large length scales, solvation is dominated by energetic effects. In this regime, large hydrophobic objects may induce a drying transition in the solvent. Further, in the small length scale regime, the excess chemical potential scales with the volume of the solute, whereas in the large length scale regime, the excess chemical potential scales with the exposed area of the solute. The crossover behavior of the solvation free energy from the wetting to the drying regime would seem to be of significance to the self assembly of biological structures [17,23]. In biological systems, the size of most hydrophobic species is such that individual species are in the wetting regime, while assemblies of such species are in the drying regime. Water may only induce a relatively weak attraction between two small hydrophobic species. When several of these species come together, however, water may induce a strong attraction between them.

The crossover behavior of the solvation free energy also implies that the strength of the interactions between the hydrophobic species, depends on the configuration of these species. The change in the interactions manifests a collective effect in the solvent, and is therefore not simply pair decomposable. Correct simulations of self assembly should capture

this collective effect, as could be done most straightforwardly with an explicit solvent model. While atomistic solvent models are highly limited for this purpose, the coarse-grained model we have developed here should prove very useful [17].

The effects of weak interactions have been ignored in this paper. Except for the movement of interfaces, which may be affected by small forces, weak interactions are not expected to induce large structural effects. Nevertheless, their inclusion will be important for quantitative studies. The inclusion of weak interactions may be accomplished by augmenting Eq. (6). Along with the constraint factor associated with the hard core of the solute, the presence of a weak attractive potential, $\phi(\mathbf{r})$, between solute and solvent, will introduce the additional factor $\exp[-\beta \int d\mathbf{r} \phi(\mathbf{r})]$. All the analysis carried out subsequent to Eq. (6) may be similarly performed in the presence of this factor. Electrostatic interactions may also be incorporated, but with somewhat greater complexity. In this case, liquid cells (with $n_i = 1$), must also possess a local polarization or dipole field \mathbf{m}_i . This vector field is Gaussian to a reasonable approximation [24] and therefore may also be integrated out. These extensions of the current model are left to future work.

ACKNOWLEDGMENTS

This work has been supported in its initial stages by the National Science Foundation (Grant Nos. 9508336 and 0078458) and in its final stages by the Director, Office of Science, Office of Basic Energy Sciences, of the U.S. Department of Energy (Grant No. DE-AC03-76SF00098).

-
- [1] K. Lum, D. Chandler, and J.D. Weeks, *J. Phys. Chem. B* **103**, 4570 (1999).
- [2] G. Hummer, S. Garde, A.E. García, A. Pohorille, and L.R. Pratt, *Proc. Natl. Acad. Sci. U.S.A.* **93**, 8951 (1996).
- [3] G.E. Crooks and D. Chandler, *Phys. Rev. E* **56**, 4217 (1997).
- [4] J.K. Percus and G. J. Yevick, *Phys. Rep.* **110**, 1 (1958).
- [5] M.S. Wertheim, *Phys. Rev. Lett.* **10**, 321 (1963).
- [6] J.L. Lebowitz and J.K. Percus, *Phys. Rev.* **144**, 251 (1966).
- [7] M.S. Wertheim, *J. Chem. Phys.* **55**, 4291 (1971).
- [8] L.R. Pratt and D. Chandler, *J. Chem. Phys.* **67**, 3683 (1977).
- [9] D. Chandler and H.C. Andersen, *J. Chem. Phys.* **57**, 1930 (1972).
- [10] K.S. Schweizer and J.G. Curro, *Phys. Rev. Lett.* **58**, 246 (1987).
- [11] D. Chandler, *Phys. Rev. E* **48**, 2898 (1993).
- [12] J.D. Weeks, K. Katsov, and K. Vollmayr, *Phys. Rev. Lett.* **81**, 4400 (1998).
- [13] D. Chandler, *Introduction to Modern Statistical Mechanics* (Oxford University Press, New York, 1987).
- [14] D.M. Huang, P.L. Geissler, and D. Chandler, *J. Phys. Chem.* (to be published).
- [15] J.S. Rowlinson and B. Widom, *Molecular Theory of Capillarity* (Clarendon, Oxford, 1982).
- [16] We have compared this approximation with seemingly more accurate approximations that include more basis sets. The comparisons indicate, however, that the approximation of one basis function per solute is accurate.
- [17] P.R. ten Wolde and D. Chandler (unpublished).
- [18] G. Hummer, S. Garde, A.E. García, M.E. Paulaitis, and L.R. Pratt, *J. Phys. Chem. B* **102**, 10 469 (1998).
- [19] A.H. Narten and D. Levy, *J. Chem. Phys.* **55**, 2263 (1971).
- [20] D.M. Huang and D. Chandler, *Phys. Rev. E* **61**, 1501 (2000).
- [21] S. X. Sun, *Phys. Rev. E* (to be published).
- [22] G.M. Torrie and J.P. Valleau, *Chem. Phys. Lett.* **28**, 578 (1974).
- [23] D.M. Huang and D. Chandler, *Proc. Natl. Acad. Sci. U.S.A.* **97**, 8324 (2000).
- [24] X. Song, D. Chandler, and R.A. Marcus, *J. Phys. Chem.* **100**, 11 954 (1996).